Nanoscale

Accepted Manuscript

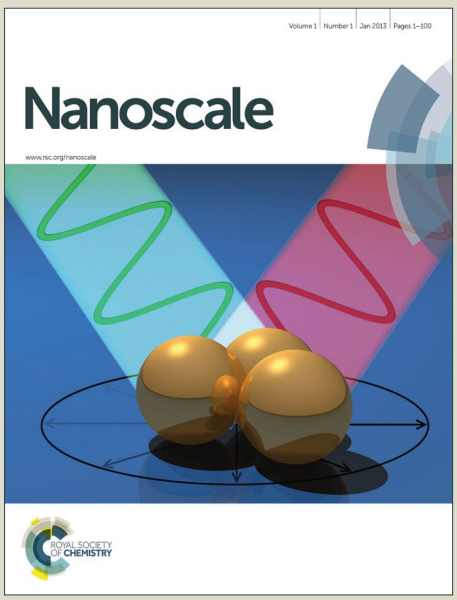

ROYAL SOCIETY OF CHEMISTRY

www.rsc.org/nanoscale

Bright, Efficient, and Color-stable Violet ZnSe-Based Quantum Dots Light-Emitting Diodes

*Aqiang Wang,[1] Huaibin Shen,[*1, 2] Shuaipu Zang, [1] Qingli Lin,[1] Hongzhe Wang,[1,2] Lei Qian,[1] Jinzhong Niu[1] and Lin Song Li[*1,2]*

[1] Key Laboratory for Special Functional Materials of Ministry of Education, Henan University, Kaifeng 475004, China

[2] Collaborative Innovation Center of Nano Functional Materials and Applications, Henan Province, P. R. China

E-mail: shenhuaibin@henu.edu.cn, lsli@henu.edu.cn.

ABSTRACT

In this paper, highly stable violet-blue emitting ZnSe/ZnS core/shell QDs have been synthesized by a novel "low temperature injection and high temperature growth" method. The resulting nearly monodisperse ZnSe/ZnS core/shell QDs exhibit excellent characteristics such as high color saturation (typical spectral full width at half-maximum between 12 and 20 nm), good emission tunability in the violet-blue range of wavelength from 400 to 455 nm, high absolute PL quantum yield (up to 83 %), and superior chemical and photochemical stability. By employing ZnSe/ZnS core/shell quantum dots (QDs) as emitters with a fully solution processable method, bright, efficient, and color-stable violet Cd-free quantum dot-based light-emitting diodes (QD-LEDs) with maximum luminance up to 2632 cd/m^2 and peak EQE at 7.83 % have been demonstrated successfully. Considering the factors of the photopic luminosity function, the brightness and efficiency results of such violet QD-LEDs not only represent 12-fold increase in device efficiency and extraordinary 100 times increase in luminance compared with previous Cd-free QD-LEDs but also can be much superior to the best performance (1.7 %) of their Cd-based violet counterparts. These results demonstrate significant progress in short-wavelength QD-LEDs and shed light on the acceleration of commercial application of environmental-friendly violet QD-based displays and lighting.

TOC Figure

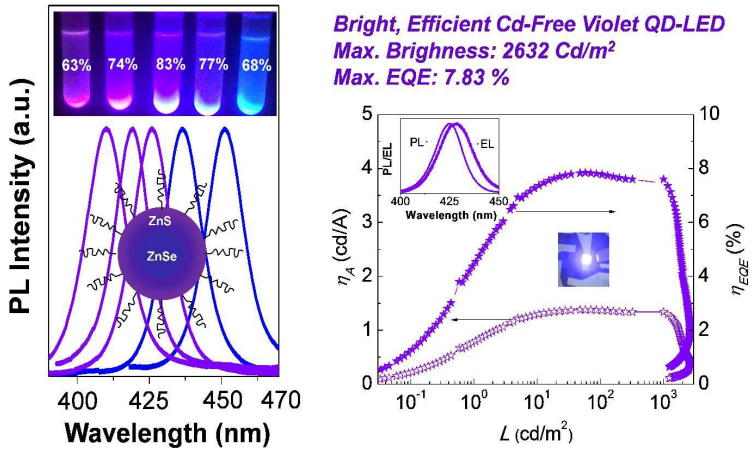

Introduction

Colloidal semiconductor quantum dots (QDs) have attracted much attention due to their unique size-dependent optical properties which can achieve excellent spectral purity at high optical flux. Their excellent optical properties make them potential superstars in light-emitting diodes (LEDs) and displays.[1-7] To fully exploit the potential of QDs in these applications, researchers need to synthesize materials that simultaneously meet the following five criteria: narrow and symmetric emission spectra, high photoluminescence (PL) quantum yields (QYs), high optical stability, eco-friendly materials, and low-cost methods for mass production. Most of previous works on highly emissive and color-tunable QDs have been mainly concentrated on materials containing toxic cadmium, mercury, or lead.[8-16] For example, red light emitter of CdSe/CdS QDs with QYs up to 90 %,[14] green region emitter of CdSe/ZnS/CdSZnS QDs with the best QYs of 100 % and improved photo- and chemical-stabilities,[15] and the QYs of $Zn_xCd_{1-x}S$/ZnS QDs also reached almost unit even in the violet-blue region.[16] However, the increasing concerns that these toxic materials such as cadmium, lead, and mercury would pose serious threats to human health and the environment, and the European Union's Restriction of Hazardous Substances (RoHS) rules ban consumer electronics containing any more than trace amounts of these materials.[17] The likelihood of commercial success for quantum dots-based light-emitting diodes (QD-LEDs) and displays will therefore be greatly improved if the devices can be fabricated using eco-friendly and heavy-metal-free QDs.

Most of the synthesis of non-toxic or low toxicity QDs are now focused on I-III-VI semiconductors (such as $CuInS_2$),[18-22] III-V semiconductors (such as InP),[23-26] and II-VI semiconductors (such as ZnSe and related Cu-, Mn-doped ZnSe),[27-31] which have low toxicity, tunable emissions in the visible to near infrared region. The current QYs for the $CuInS_2$ core/shell QDs is up to 60 %, but the emission tunability is mainly confined between 540 and 650 nm.[20, 21] The obtained III-V heavy-metal-free QDs typically possess emissions from 480 to 600 nm with the highest QYs up to 70 %.[24, 25] Most recently, the QD-LEDs fabricated based on low toxicity QDs also have some progress. The maximum brightness utilizing I-III-VI semiconductor QDs have reported over 1000 cd/m^2 in yellow-red area without the

demonstration of external quantum efficiency (EQE).[21, 32] For those using the III-V heavy-metal-free QDs, such as InP/ZnSeS QDs, the maximum EQE can reach more than 3 % with electroluminescence (EL) peak at 518 nm and show full width at half-maximum (FWHM) of about 64 nm.[33] These results demonstrate good color tunability and competitive efficiencies for heavy-metal-free QD-LEDs in the range of 510 to 630 nm, but still lack of good result on the violet-blue emission QD-LEDs due to the absence of corresponding heavy-metal-free QD emitters. Therefore, one of the main challenges is the development of efficient violet-blue emitters and the realization of higher efficiency QD-based LEDs by using heavy-metal-free QDs.

So far, for the heavy-metal-free QDs, no matter I-III-VI or III-V QDs, all cannot obtain high QYs (>70 %) and high stability QDs in the violet-blue area, let alone high brightness and efficiency of corresponding violet-blue QD-LEDs. Most recent studies have begun to concentrate on the synthesis of wide bandgap ZnSe QDs as potential violet-blue emitter. Our previous report showed an impressive high QY of 70 %,[30] but the stability of ZnSe related QDs is still unsatisfied. Previously reported red-green and Cd-containing blue QD emitters showed QYs of up to 90 % with high stabilities,[14-16] and these results all indicate the immediacy of the QY and stability improvement of violet-blue ZnSe QDs. Therefore, the synthesis of violet-blue QDs which can simultaneously satisfy high PL QYs (> 80 %), narrow and symmetric emission (FWHM < 20 nm), high stability, environmentally friendly, and low-cost is an urgent demand in the realization of heavy-metal-free violet-blue and thus full-color QD-LEDs. Herein, we present a method for the synthesis of violet-blue emitting ZnSe/ZnS core/shell QDs that show high QYs as well as high stability. Different from most of the traditional nucleation at high temperature/shell growth at low temperature method, we adopt a lower temperature injection and higher temperature growth method for the synthesis of ZnSe/ZnS core/shell QDs.[14-16] Nearly monodisperse ZnSe/ZnS core/shell QDs were synthesized with high absolute PL QYs (up to 80 %), high color purity (with FWHM about 12~20 nm), good color tunability in the violet-blue range from 400 to 455 nm. Significantly, such ZnSe/ZnS core/shell QDs showed very good chemical/photochemical stability compared with previous studies.[27, 30]

Furthermore, violet QD-LEDs using ZnSe/ZnS core/shell QDs have also been successfully demonstrated with a fully solution-processed method. Highly bright violet QD-LEDs show maximum luminance of 2632 cd/m^2 and peak EQE of 7.83%. And in a sense, such brightness and efficiency exhibit the huge superiority to those of the best Cd-based violet-blue QD-LEDs considering the factors of the photopic luminosity function. These results may offer a practicable platform for the realization of heavy-metal-free QDs based violet-blue and full-color displays and lighting.

Experimental Section

Chemicals: All reagents were used as received without further experimental purification. Zinc oxide (ZnO, 99.99% powder), sulfur (S, 99.98%, powder), 1-octadecene (ODE, 90%), oleic acid (OA, 90%), octanethiol (OT, 98%), zinc acetate (99.99 %), dimethyl sulphoxide (DMSO, 99.7%), tetramethylammonium hydroxide (TMAH, 97%), and selenium (Se, 99.99%, powder) were purchased from Aldrich. Chlorobenzene (analytical grade), hexanes (analytical grade), paraffin oil (analytical grade), and methanol (analytical grade) were obtained from Beijing Chemical Reagent Ltd., China.

Typical Synthesis of ZnSe/ZnS with Low Temperature Nucleation/ High Temperature Shell Growth Method: *Stock solution for Zn precursor:* A mixture (20 mL in total) of ZnO (0.488 g, 6 mmol), oleic acid (18 mmol, 5.076 g), and 14 mL paraffin oil were loaded in a 100 mL three-necked flask and heated to 300 ºC under nitrogen to obtain a clear solution. Zn precursor solution was stored at 120 ºC for the following use. *Stock solution for Se precursor:* Se (0.237 g 3 mmol) and 30 mL of ODE were mixed in a 100 mL three-necked flask. Under nitrogen flow and stirring, the mixture was heated to 220 ºC for 180 min, and then the reaction solution was cooled down to room temperature. Se precursor solution was stored at 50 ºC for the following use. *Synthesis of ZnSe QDs with lower temperature and synthesis of ZnSe/ZnS core/shell QDs with high temperature:octanethiol as S precursor and ligands for the synthesis of ZnSe/ZnS core/shell QDs:* ZnSe core was prepared according to the previous literature of our group (see Supporting Information).[30] In a typical synthesis, 2 mL Se precursor and 8 mL paraffin oil were heated to 300ºC under nitrogen flow in a 100 mL flask. Next, 1.3 mL Zn precursor solution was injected

and maintained for 5 min for the formation of ZnSe core QDs (Figure S1 and Figure 1a). Subsequently, the reaction temperature was set at 320 ºC without any purification steps, then 2 mL OT mixed with 20 mL of Zn precursor was added at a rate of 6 mL/h. All the shell growth process lasted for 4 h. Aliquots of QDs were taken during the reaction to analyze the development of ZnSe/ZnS core/shell QDs (Figure 1). After the reaction was completed, the temperature was cooled down to room temperature and the QDs were purified using acetone or methanol. ZnSe/ZnS core/shell QDs with different shell growth temperature (as shown in Figure 3) were prepared following the same procedures as described above for the synthesis of ZnSe/ZnS core/shell QDs at 320ºC, with variation of different growth temperature of 240 ºC, 260 ºC, 280 ºC, 300 ºC, and 340 ºC, respectively (see Supporting Information). *S-ODE as S precursor for the synthesis of ZnSe/ZnS core/shell QDs:* The synthesis of ZnSe/ZnS core/shell QDs with S-ODE as S precursor was similar to aforementioned method, just octanethiol was replaced by conventional S-ODE (0.2 M) as S precursor.

Fabrication and characterization of QD-LEDs: QD-LEDs were fabricated on a patterned ITO glass substrate (25.4 mm×25.4 mm) with a sheet resistance of ~20 Ω sq^{-1} and consisting of 4 emitting spots with an active area of 4 mm^2. The substrates were washed with deionized water, acetone and isopropanol, consecutively, for 15 min each, and then treated with ozone for 15 min in air to form clean and hydrophilic surface for following spin-coating processes. PEDOT:PSS (AI 4083) was first spin-coated onto each ITO substrates followed by baking at 150 ºC for 15 min in air. The spin-coating of the poly(9-vinlycarbazole)(PVK), ZnSe/ZnS QD and ZnO nanoparticle layers were then conducted in a N_2-filled glove box. The hole-transport layer of PVK was spin-coated using 1.5 wt% in chlorobenzene (2,000 rpm for 30 s), followed by baking at 160 ºC for 30 min. ZnSe/ZnS QDs toluene solution (15 mg/mL) and ZnO nanoparticles dispersed in ethanol (30 mg/mL) were used to form emissive and electron injection layers with spin speed of 2000 rpm (layer thickness of ~25 nm) and 3000 rpm (layer thickness of ~30 nm), respectively, followed by another 30 min baking process under 75 ºC. These substrates were then transferred into a custom high-vacuum evaporation chamber (background pressure,

~3 × 10^{-7} torr) to deposit the top Al cathode (with thickness of 100 nm) patterned by an in situ shadow mask to form an active device area of 4 mm^2.

Characterization: Room temperature UV-vis absorption and PL spectra were measured with an Ocean Optics spectrophotometer (mode PC2000-ISA). The PL QYs were measured by an integrating sphere whose inner face was coated with BenFlect equipped with a spectrofluorometer. The excitation and emission bandwidths were 5.0 and 0.1 nm respectively. The step size was 0.2 nm and the integration time was 0.3 seconds. TEM observation was conducted by a JEOL JEM-2010 electron microscope with accelerating voltage of 200 kV. The thickness of the films was measured by a UVISEL 2 Scientific Spectroscopic Ellipsometer (HORIBA Scientific). The Current–luminance–voltage characteristics were measured on a Keithley 2400 sourcemeter and a Keithley 6485 picoammeter coupled with a Si photodetector (Newport UV-818), which was calibrated by a Minolta CS-100 Chroma Meter. The EL spectra were recorded using an Ocean Optics spectrometer (USB 2000) and a Keithley 2400 power source. Detailed calculations of power efficiency and external quantum efficiency are provided in the Supporting Information.

Results and Discussion

Synthesis of high QY and stable ZnSe/ZnS core/shell QDs

The ZnSe QD cores were prepared according to the previous literature of our group [30] (see Supporting Information). The temporal evolution of the absorption and PL spectra of the ZnSe QDs are shown in Figure S1 with the reaction temperature of 300 ºC. The as-synthesized ZnSe QDs showed significant PL emission in 400–450 nm range with narrow FWHM of 12–16 nm and absolute PL QYs of 20 to 50%. Figure 1 shows the optical spectra of ZnSe core (corresponding to Figure S1-5 min, with QY of 41%) and ZnSe/ZnS core/shell QDs (see the Experimental Section for details) taken at different reaction time with the reaction temperature of 320 ºC. The FWHM of PL spectrum of the ZnSe core was about 18 nm (Figure 1A). The shell formation process was triggered by the addition of octanethiol as S precursor and

Zn-OA as Zn precursor, and the PL QYs of core/shell structured QDs were sharply increased with stable narrow FWHM (< 20 nm). When the reaction lasted for 4 h, the measured QY reached as high as 83 %, which is the highest value of ZnSe/ZnS QDs reported so far. A little blue-shift in PL indicates partial formation of ZnSeS alloy shells, which is considered as opposite tendency to the formation of core/shell QDs by the epitaxial growth of ZnS shell with high temperature nucleation and low temperature shell growth method. [22]

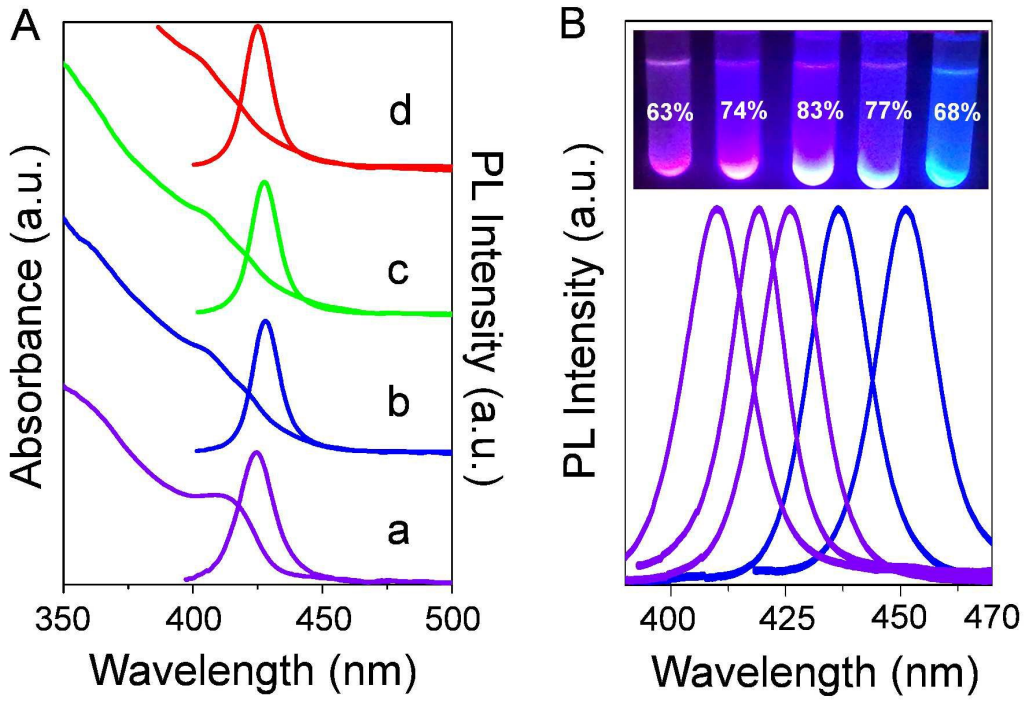

Figure 1. (A). Evolution of the absorption and PL spectra upon consecutive growth of ZnSe/ZnS core/shell QDs. a: ZnSe core, and ZnSe/ZnS obtained after the growth of ZnS shell for b: 1h, c: 2h, and d: 4h, respectively. (B) Normalized PL spectra of ZnSe/ZnS core/shell QDs (dispersed in hexanes) starting from different ZnSe cores with tunable PL peaks covering from 400 to 455 nm (λ_{ex}= 360 nm), and representative emission colors of ZnSe/ZnS core/shell QDs (in hexanes) under the radiation of a UV lamp.

There are two proposed reasons for the obtaining of core/shell QDs with such high QYs. One is the growth of shells at high temperature. Different from traditional nucleation at high temperature/shell

growth at low temperature method,[34] our preparation approach adopted shell growth at a high temperature level. We speculate that the significantly improved PL QYs and stability observed here is at least partially caused by the highly crystalline shell that results from high-temperature mild shell-growth conditions (a detailed discussion will be given later). Another one lies in the successful surface passivation of the cores with wider bandgap capping materials. When the ZnS shells are grown onto ZnSe QDs, the newly formed ZnSeS shell and ZnS shell can structurally passivate the surface defects of cores and energetically confine the excitons in the cores due to the wider bandgap of shell materials. All of the above facilitates the great improvement of the PL QYs. Figure 1B clearly demonstrates the PL tunability of ZnSe/ZnS QDs which were prepared using different ZnSe cores in the wavelength range of 400–455 nm. This covers most part of the violet-blue spectral range which is very important for the application of violet-blue LEDs.

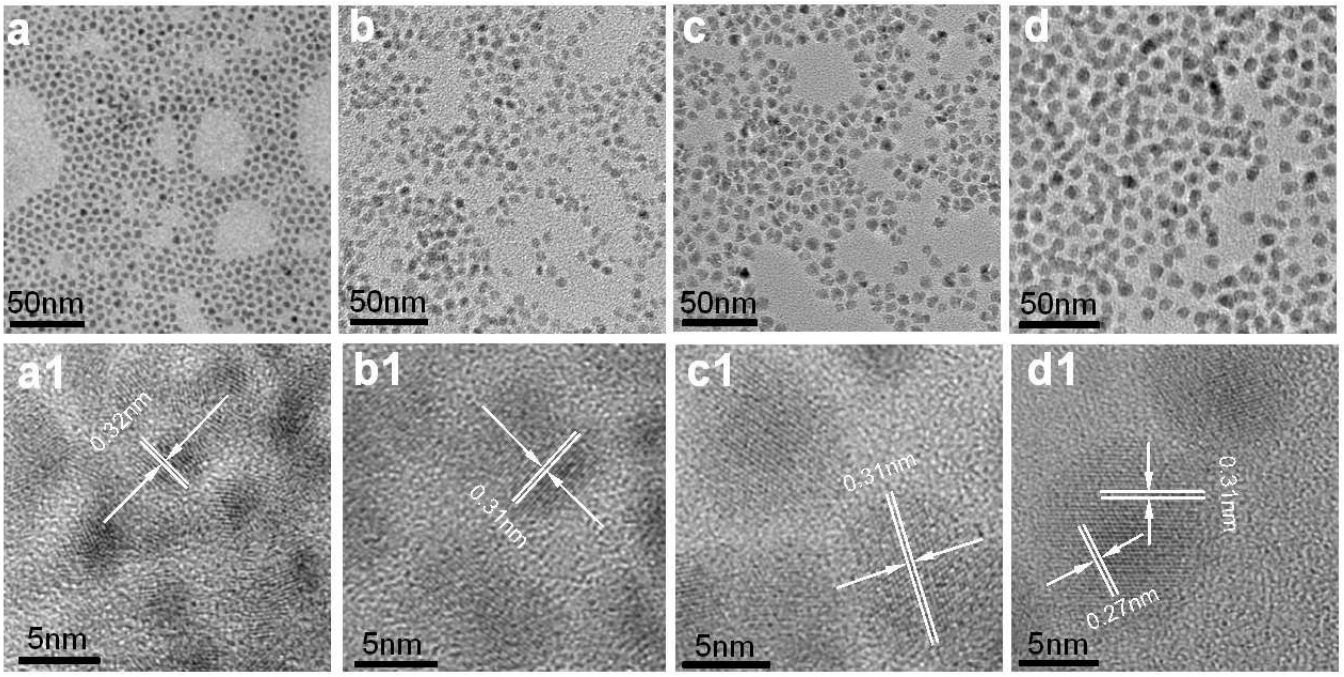

Figure 2. TEM images of the ZnSe cores (a) and ZnSe/ZnS core/shell QDs obtained after shell growth time of 1 h (b), 2 h (c), and 4h (d), respectively; a1, b1, c1, and d1 show the corresponding HRTEM of a, b, c, and d, respectively.

Figure 2 shows the TEM and HRTEM results of ZnSe cores and ZnSe/ZnS core/shell QDs obtained after ZnS shell coating. All the TEM images show well-controlled size and size distributions with average particle diameters of 7.6 nm (b), 8.7 nm (c), and 10 nm (d) for ZnSe/ZnS QDs obtained with different shell growth time but the same batch of original ZnSe core QDs (a), which have a mean diameter of 4.5 nm. The corresponding HRTEM images of ZnSe cores and ZnSe/ZnS core/shell QDs are shown in Figure 2 a1-d1. Those HRTEM images show continuous lattice fringes throughout the whole particles and this reveals the high crystalline nature of as-synthesized ZnSe and ZnSe/ZnS QDs. No evidence for the formation of an interface between ZnSe core and ZnS shell can be detected (the lattice mismatch between ZnSe and ZnS is about 5%), which implies the coherent epitaxial growth of shells.[34] To further characterize the evolution of structures of ZnSe/ZnS core/shell QDs, their crystallographic properties were determined by XRD (Figure S2). According to the XRD patterns, the peak positions of the ZnSe QDs are in agreement with bulk ZnSe in zinc blende structure (JCPDS No. 80–0021). An obvious peak shift to the position of standard zinc blende phase ZnS (JCPDS No. 80–0020) also has been observed when ZnS shells were grown onto the ZnSe cores and all samples still kept cubic structures.

Low temperature nucleation/high temperature shell growth method

To get high QYs and stable ZnSe/ZnS QDs, the growth of shell materials is conducted at high temperature, which is different from the traditional high temperature nucleation/ low temperature shell growth method.[34, 35] It is widely accepted in the synthesis of core/shell structured QDs that cores should be crystallized under elevated temperatures and the shell growth process should be conducted in comparatively low temperature to stop the separate nucleation of shell precursor.[35] In principle, a high shell growth temperature may lead to a new nucleation with shell material after the injection of precursors, but the concentration of shell precursor nucleation should reach Lamer nucleation concentration. If the precursor concentration can be controlled beneath the super-saturation level,[36] such as lower the added amount of precursors or using low activity and mild precursors, nucleation process will therefore be suppressed. So, mere growth of shells at higher temperature is completely possible.

Based on this envisage, Zn-OA and octanethiol were used as Zn and S precursors for shell growth at high temperature. No new ZnS QDs were formed during the slow addition of precursors, and the quality of as-prepared ZnSe/ZnS core/shell QDs is evidently superior to similar core/shell QDs synthesized through low temperature shell growth strategy in PL quantum yield (up to 83 %) and color purity (FWHM about 12 – 20 nm).

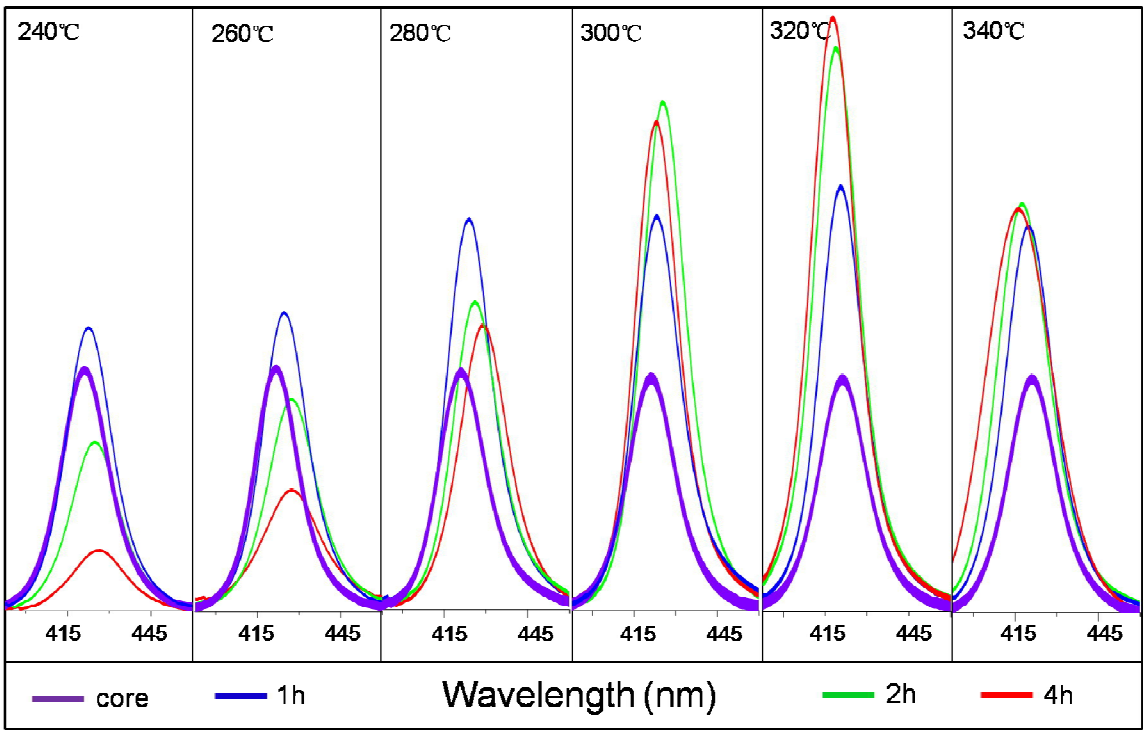

Figure 3. Evolution of PL spectra of ZnSe/ZnS core/shell QDs with different shell growth time and temperatures. Note: Same batch of ZnSe QDs (PL at 424 nm) have been selected as starting cores for the shell growth.

In order to prove the advantage of this method, ZnSe/ZnS core/shell QDs were specially synthesized using the same batch of ZnSe cores under different shell growth temperatures. Figure 3 shows the PL spectra of ZnSe/ZnS core/shell QDs with different shell growth time and temperature but same ZnSe cores. The detailed information of QYs, PL peaks, and FWHMs with different shell growth time and temperatures are summarized in Table S1. The PL intensities showed a sharp increase at the initial stage (such as in 1 h) when the growth temperature was set at 280 °C and lower, but the QYs kept dropping

after the shell growth time was longer than 2 h. The PL QYs dropped from 48 % (1 h) to 37 % (2 h) and 60 % (1 h) to 51 % (2 h) when the growth temperature was set at 240 °C and 280 °C, respectively. When the temperature was increased to 320 °C for the growth of shell material, the absolute QYs of final ZnSe/ZnS core/shell QDs could be kept up over 83 %, and the FWHM of PL decreased from 18 nm (ZnSe core) to 16.6 nm (at the end of the reaction), which was consistent with the narrowing of size distribution of QDs. This narrow PL FWHM is most likely the result of the matching between the slow infusion rate of shell precursors and the low reactivity of octanethiol, which ensures the constant epitaxial growth of ZnS shell and is consistent with recent researches. [14, 37] Such superior optical properties can be attributed to the successful surface passivation of the ZnSe cores with wider bandgap ZnS shells. But it is more essential for the growth of shell material at high temperature, which can promote the diffusion of S and Zn atoms into the ZnSe cores, and thus ensures the formation of ZnSeS transition layer between ZnSe core and ZnS shell (which can be proved from the blue shift of PL peaks). The ZnSeS shells can structurally passivate the surface dangling bonds of cores and energetically confine the excitons in the cores and also make consecutive transition of lattice parameters from core to shell, which is critical for the reduction of structural defects. However, when the growth temperature is too high, such as 340 °C, high QY can be maintained but the PL FWHM is broadened rapidly with the increase of reaction time which leads to the decline of the quality of final QDs.

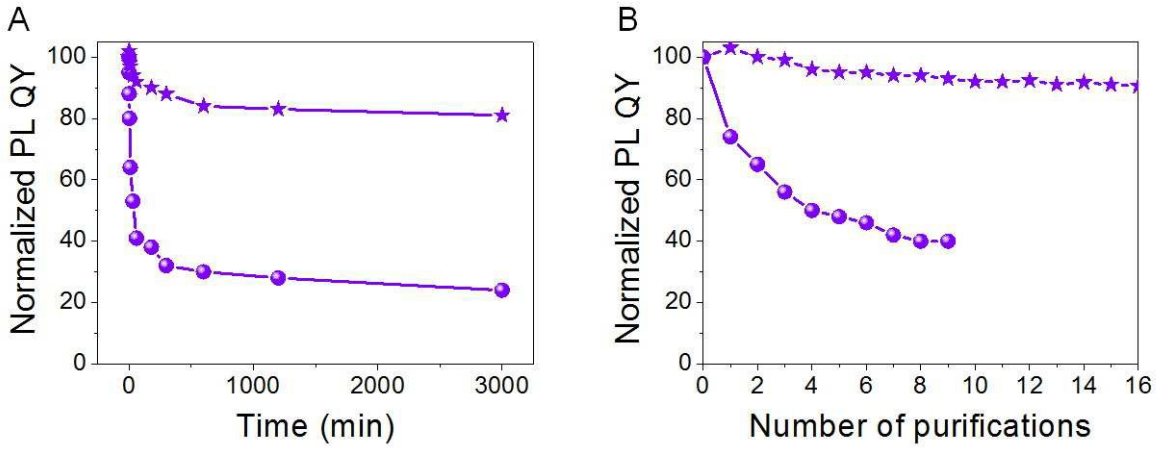

Figure 4. Evolution of the relative PL stability of ZnSe/ZnS core/shell QDs which synthesized with octanethiol (★) and conventional S-ODE (●) as S precursor, respectively. (A) Photochemical stability of

QDs in hexanes solution under UV-irradiation (12 W, 365 nm); (B) Stability of QDs upon repeated purification process steps.

It should be mentioned that choosing octanethiol stock solution instead of conventional S-ODE as S precursor is not just because it can improve the QYs of ZnSe/ZnS QDs, but more importantly, octanethiol as ligand can bind strongly to the QD surface and thus enhance their stability under UV-irradiation and repeated purification process (Figure 4, Figure S3). Figure 4A shows that the ZnSe/ZnS core/shell QDs synthesized with octanethiol are very stable, and the absolute QY can be maintained more than 80 % of its primary value even after 3000 min while the ZnSe/ZnS core/shell QDs synthesized using conventional S-ODE reduced to below 30% of their initial value. It is also clearly shown in Figure 4B, the QYs of ZnSe/ZnS core/shell QDs which were synthesized with octanethiol as S precursor show a slightly decline upon many cycles of purification in hexanes (see Supporting Information). But the QY of ZnSe/ZnS core/shell QDs which were synthesized with S-ODE as S precursor dropped to below 40% of their initial value only after 10 times of precipitation and it was almost not dispersable in hexanes after 10 times precipitation. The detailed performance comparison and discussion of QD-LEDs fabricated using ZnSe/ZnS QDs synthesized with different S sources (*i.e.* S-ODE and octanethiol) will be given later.

Fabrication of Cd-free violet emitting LEDs using ZnSe/ZnS core/shell QDs as emitters

It is known that violet (380–440 nm) radiation has been widely used in many applications, such as sterilization, drinking water purifiers, phototherapy, and photocopying.[38] With the renovating of synthetic method, although violet QDs with high QYs have been continuously developed, but there are few researches about violet QD-LEDs. Based on recent published results, the best luminance of Cd-based violet-blue QD-LEDs can reach up to 2250 cd/m^2 with EL peak at 437 nm and EQE about 1.7 %.[6] Ji *et al* [39] fabricated the deep-blue QD-LEDs using ZnSe/ZnS core/shell QDs with an inverted device architecture, the EL emission peak of the deep-blue QD-LEDs is 441 nm with maximum luminance and current efficiency reaching 1170 cd/m^2 and 0.51 cd/A, respectively. However, the inverted structure QD-LEDs cannot be fully solution-processable, since the solution processing of organic hole injection layer

and following QD deposition would cause a destructive interlayer mixing. Violet emitting devices based on cadmium-free ZnSe/ZnS core/shell QDs have been demonstrated by So and Wedel groups with and without fully solution-processed devices respectively, and the maximum luminance of 25 cd/m^2 or EQE was about 0.65 %.[40, 41] The reasons for low efficiency of violet QD-LEDs mainly lie in the following two points. The first is the relatively low QYs of violet QDs. Second, larger potential energy barrier between the violet-blue QDs and hole transport polymer, which would result in low hole injection efficiency along with poor EQE. The reason for low brightness of violet QD-LEDs mainly lies in the photometric quantity of luminance, which is determined by the relative sensitivity of human vision to different wavelengths, shows much lower spectral perception sensitivity for violet light versus green and red counterparts.

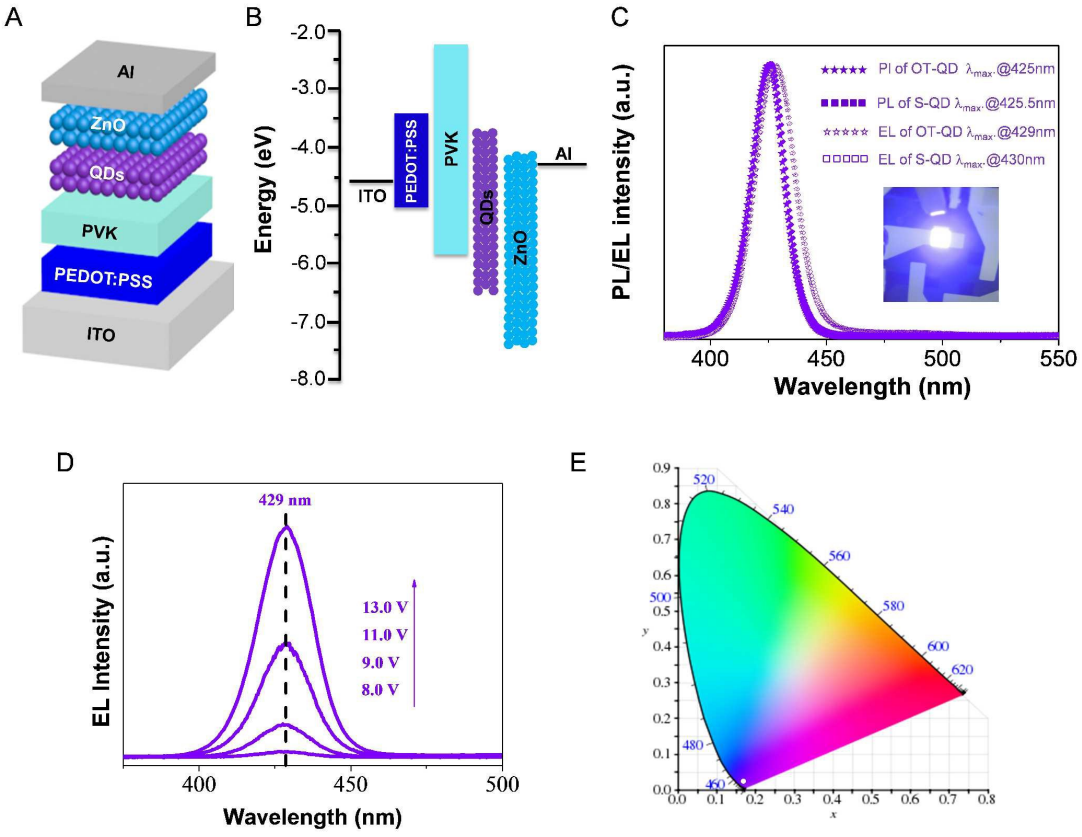

Figure 5. (A) Schematic of layered QD-LEDs device. (B) Energy level diagram for the various layers. (C) Normalized PL spectra of ZnSe/ZnS core/shell QDs with octanethiol (OT-QD for short) and S-ODE (S-QD for short) as S sources, and corresponding EL spectra of violet QD-LED. Inset: Electroluminescent image under an applied voltage of 11 V. (D) Evolution of EL spectra of QD-LEDs

with increasing bias voltage. (E) CIE color coordinates of (0.169, 0.023) corresponding to the violet emission spectra in (C).

Based on this efficient synthesis method and resultant high quality violet ZnSe/ZnS core/shell QD emitters, all solution-processed violet QD-LEDs were fabricated to further explore their potential application in fields of EL devices driven by low DC voltage. Different from our previous reports which using (poly[9,9-dioctylfluorene-co-N-[4-(3-methylpropyl)]-diphenylamine] (TFB) as HTLs, [16, 42, 43] poly-N-vinylcarbazole (PVK) was chosen as the hole-transporting material and ZnO was used as the electron-transporting layers. Due to their higher HOMO levels, TFB cannot provide efficient hole injection pathway and are not suitable for HTLs in high-quality violet QD-LEDs. PVK has a lower HOMO energy level (− 5.8 eV) compared to that of TFB (− 5.3 eV), which may inevitably facilitate the efficient injection of holes. The spectral overlap between PVK emission and ZnSe/ZnS absorption can efficiently improve the transfer of excitons formed on PVK to QDs (Supporting Information, Figure S4). For the injection of electrons, ZnO (with an electron affinity of ~4.3 eV and an ionization potential of ~7.6 eV) NP layer was adopted as electron injection layer (ETL) to form an efficient injection channel of electron and help to block holes in the QD layer due to the large valence band offset at the QD-ZnO interface. [4, 42] The choices of HTL and ETL ensure the efficient injection of holes and electrons, which lead to an improved charge recombination within QD layer. The structure of the QD-LEDs is schematically shown in Figure 5A and the corresponding schematic energy level diagram is shown in Figure 5B. The QD-LEDs were fabricated with layers of indium tin oxide (ITO)/poly (ethylenedioxythiophene):polystyrene sulphonate (PEDOT:PSS) (40 nm)/ PVK (30 nm)/ZnSe/ZnS core/shell QDs (25 nm)/ZnO NPs (30 nm)/Al to confine exciton formation within the QD layer. Surface SEM images of uniformly, compactly packed emitting layer of ZnSe/ZnS QDs and electron transport layer of ZnO NPs are shown in Figure S5, The cross-sectional SEM image of ITO/PEDOT:PSS/PVK/QDs /ZnO is shown in Figure S6 and the thickness of each layer in the device are consistent with the results measured by ellipsometer. Figure 5C shows the PL spectra of ZnSe/ZnS core/shell OT-QDs (in toluene) and the EL spectrum of the corresponding QD-LEDs, respectively. As can be seen from Figure 5C, the color purity of EL is in good

agreement with PL of the ZnSe/ZnS QDs with a little increase in the FWHM from 16.6 nm to 20.4 nm. The EL peak of the violet QD-LEDs locates at 429 nm which shows a slight red-shift compared with the PL peak, and no noticeable parasitic emission from adjacent organic layers can be observed during the device operation, which supports the effective suppression of exciton leakage from the emissive QD layer. Figure 5D shows the EL spectra of the ZnSe/ZnS based QD-LEDs measured at voltages from 8 V to 13 V, and we noticed that the FWHM (~20.5 nm) of EL spectra remains nearly unchanged during all these tests. The corresponding EL spectra at half-exponential coordinates were shown in Figure S7 (see Supporting Information), which proved no noticeable emissions from deep-level trap states or EL emissions from the adjacent organic layers. The Commission Internationale de l'Eclairage (CIE) chromaticity coordinates of the EL spectra of the QD-LEDs is shown in Figure 5E, which shows identical coordinates of (0.169, 0.023) in the pure violet territory.

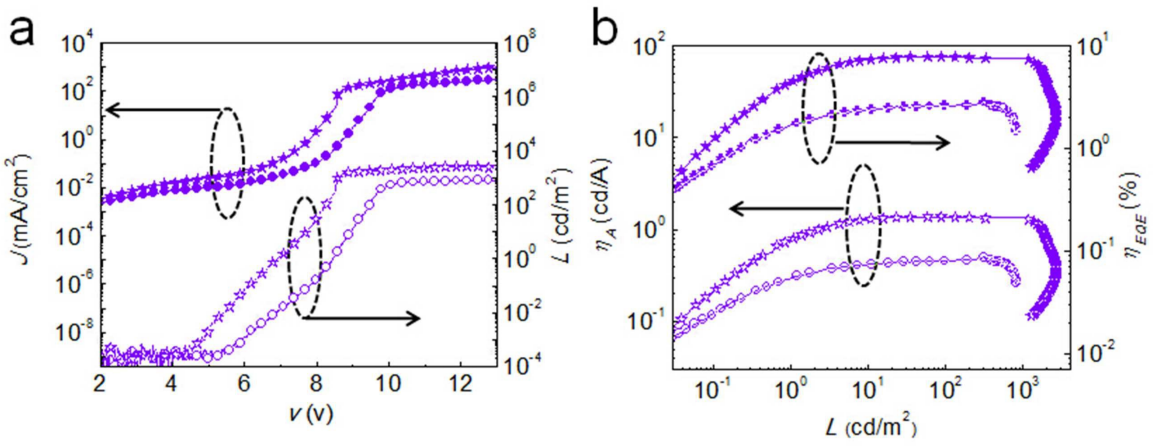

Figure 6. EL performance of QD-LEDs with violet emissions based on ZnSe/ZnS core/shell QDs which synthesized with octanethiol (★) and conventional S-ODE (●) as S precursor. (a) Current–density (J) and luminance (L) versus driving voltage (V), (b) Current efficiency (η_A) and external quantum efficiency (EQE) versus luminance.

Figure 6 shows the direct comparison of current density–luminance–voltage (J–L–V) characteristics, luminous efficiency, and EQE curves for violet QD-LEDs fabricated with S sources of octanethiol (OT-QD for short) and S-ODE (S-QD for short), respectively. These QDs represent two kinds of violet

ZnSe/ZnS QDs with similar synthesis procedure and emission wavelength, which ensured the comparability of corresponding EL performance to prove the superiority of octanethiol as S source. The absolute QYs of final ZnSe/ZnS core/shell S-QDs could be kept up over 48 % with PL peak at 425.6nm, the FWHM of PL and EL are 17.2 nm and 21.6 nm, respectively (Figure 5C). The violet QD-LEDs based on our ZnSe/ZnS core/shell QDs showed similar EL peak of 429 nm and 430 nm for OT-QD and S-QD (Figure 5C and Figure 5D), respectively, and high brightness with maximum value of 804 cd/m^2 (for S-QD@12.8 V) and 2632 cd/m^2 (for OT-QD@12.1 V) were recorded (Figure 6a). It is note-worthy that the peak luminance obtained by using OT-QDs represents the highest level of brightness reported so far for heavy- metal-free QD-based violet LEDs. Considering the different conversion factors from photopic luminosity function for different wavelength (for examples, 430 nm-0.0116, 440 nm-0.023, 470 nm-0.091, 535 nm-0.9148, 610 nm-0.503), emission with peak of 430 nm corresponds a 1/40, 1/80, and 1/8 of sensitivity of human vision of red, green, and blue ones, respectively. Thus, 2632 cd/m^2 at 429 nm is really a high value than that of previously reported heavy-metal-free QD-LEDs in more than 100 times.[35] In Figure 6a, QD-LEDs with OT-QDs show higher current density that those using S-QDs, which indicates that shorter surface capping ligand of OT favors the charge injection than longer capping molecules such as OA. The QD-LEDs using S-QDs show their highest EQE of 2.6 % (Figure 6b), current efficiency of 0.46 cd/A (Figure 6b), and power efficiency of 0.15 lm/W (Figure S8), respectively. While control devices using OT-QDs exhibit record values of maximum EQE of 7.83 % (Figure 6b), current efficiency of 1.38 cd/A, (Figure 6b) and power efficiency of 0.53 lm/W (Figure S8) for violet QD-LEDs based on heavy-metal-free QDs. Such high efficiency is 4 times more than the best violet Cd-containing QD-LEDs technology (EQE=1.7 %).[6] This high quality violet QD-LEDs are originating from the high QYs of the ZnSe/ZnS core/shell QDs and the excellent structure design of QD-LEDs. The optimized selection of organic PVK hole injection layer and inorganic ZnO electron injection layer can effectively guarantee good energy band alignment between layers and thus the matching injection rates of carriers.

Conclusions

In summary, we introduce the concept of low temperature nucleation and high temperature shell growth to synthesize high-quality violet-blue emitting ZnSe/ZnS core/shell QDs. The resulting nearly monodisperse ZnSe/ZnS core/shell QDs exhibit excellent characteristics such as high stable PL QY up to 83%, superior color saturation with FWHM < 20 nm, and flexible emission tunability at wavelength range of violet-blue from 400 to 455 nm. Highly bright and efficient violet QD-LEDs demonstrate maximum luminance up to 2632 cd/m^2 with peak EQE of 7.83% successfully by using such ZnSe/ZnS core/shell QD emitters. These results may offer a practicable platform for the realization of heavy-metal-free QD-based violet lighting devices.

Acknowledgments. The authors gratefully acknowledge the financial support from the research project of the National Nature Science Foundation of China (21201055 and 61474037), Program for Science & Technology Innovation Talents in University of Henan Province (No. 14HASTIT009), and Program for Changjiang Scholars and Innovative Research Team in University (No. PCS IRT1126).

REFERENCES

1. V. L. Colvin, M. C. Schlamp, A. P. Alivisatos, *Nature,* **1994**, *370*, 354.
2. S. Coe, W. K. Woo, M. G. Bawendi, V. Bulović, *Nature,* **2002**, *420*, 800.
3. Q. Sun, Y. A. Wang, L. S. Li, D. Wang, T. Zhu, J. Xu, C. Yang, Y. Li, *Nat. Photonics,* **2007**, *1*, 717.
4. L. Qian, Y. Zheng, J. Xue, P. H. Holloway, *Nat. Photonics,* **2011**, *5*, 543.
5. S. Kim, S. H. Im, S.-W. Kim, *Nanoscale,* **2013,** *5,* 5205.
6. J. Kwak, W. K. Bae, D. Lee, I. Park, J. Lim, M. Park, H. Cho, H. Woo, D. Y. Yoon, K. Char, S. Lee, C. Lee, *Nano Lett*., **2012**, *12*, 2362.
7. K. H. Lee, J. H. Lee, W. S. Song, H. Ko, C. Lee, J. H. Lee, H. Yang, *ACS Nano,* **2013**, *7*, 7295.
8. W. Zhang, H. Zhang, Y. Feng, X. Zhong, *ACS Nano,* **2012**, *6*, 11066.
9. R. S. Sanchez, E. Binetti, J. A. Torre, G. Garcia-Belmonte, M. Striccoli, I. Mora-Sero,

Nanoscale, **2014,** *6,* 8551.

10. H. Shen, C. Zhou, S. Xu, C. Yu, H. Wang, X. Chen, L. S. Li, *J. Mater. Chem.,* **2011**, *21*, 6046.
11. W. K. Bae, K. Char, H. Hur, S. Lee, *Chem. Mater.,* **2008**, *20*, 531.
12. H. Shen, H. Wang, X. Chen, J. Niu, W. Xu, X. Li, X. Jiang, Z. Du, L. S. Li, *Chem. Mater.,* **2010**, *22*, 4756.
13. S. Taniguchi, M. Green, T. Lim, *J. Am. Chem. Soc.,* **2011**, *133*, 3328.
14. O. Chen, J. Zhao, V. P. Chauhan, J. Cui, C. Wong, D. K. Harris, H. Wei, H.-S. Han, D. Fukumura, R. K. Jain, M. G. Bawendi, *Nat. Mater.,* **2013**, *12*, 445.
15. S. Jun, E. Jang, *Angew. Chem. Int. Ed.,* **2013**, *52*, 679.
16. H. Shen, X. Bai, A. Wang, H. Wang, L. Qian, Y. Yang, A. Titov, J. Hyvonen, Y. Zheng, L. S. Li, *Adv. Funct. Mater*., **2014**, *24*, 2367.
17. Y. Shirasaki, G. J. Supran, M. G. Bawendi, V. Bulović, *Nat. Photonics,* **2013**, *7*, 13.
18. B. Chen, H. Zhong, M. Wang, R. Liu, B. Zou, *Nanoscale,* **2013,** *5,* 3514.
19. H. Z. Zhong, S. S. Lo, T. Mirkovic, Y. C. Li, Y. Q. Ding, Y. F. Li, G. D. Scholes, *ACS Nano,* **2010**, *4*, 5253.
20. L. Li, A. Pandey, D. J. Werder, B. P. Khanal, J. M. Pietryga, V. I. Klimov, *J. Am. Chem. Soc.,* **2011**, *133*, 1176.
21. B. Chen, H. Zhong, W. Zhang, Z. Tan, Y. Li, C. Yu, T. Zhai, Y. Bando, S. Yang, B. Zou, *Adv. Funct. Mater.,* **2012**, *22*, 2081.
22. K. Yu, P. Ng, J. Ouyang, M. B. Zaman, A. Abulrob, T. N. Baral, D. Fatehi, Z. J. Jakubek, D. Kingston, X. Xu, X. Liu, C. Hebert, D. M. Leek, D. M. Whitfield, *ACS Appl. Mater. Interfaces,* **2013**, *5*, 2870.
23. V. Brunetti, H. Chibli, R. Fiammengo, A. Galeone, M. A. Malvindi, G. Vecchio, R. Cingolani, J. L. Nadeau, P. P. Pompa, *Nanoscale,* **2013,***5,* 307.
24. K. Huang, R. Demadrille, M. G. Silly, F. Sirotti, P. Reiss, O. Renault, *ACS Nano,* **2010**, *4*, 4799.
25. L. Li, P. Reiss, *J. Am. Chem. Soc.,* **2008**, *130*, 11588.

26. J. Lim, W. K. Bae, D. Lee, M. K. Nam, J. Jung, C. Lee, K. Char, S. Lee, *Chem. Mater.,* **2011**, *23*, 4459.

27. L. S. Li, N. Pradhan, Y. Wang, X. Peng, *Nano Lett.,* **2004**, *4*, 2261.

28. K. Yu, A. Hrdina, J. Ouyang, D. Kingston, X. Wu, D. M. Leek, X. Liu, C. Li, *ACS Appl. Mater. Interfaces,* **2012**, *4*, 4302.

29. N. Pradhan, D. Goorskey, J. Thessing, X. Peng, *J. Am. Chem. Soc.,* **2005**, *127*, 17586.

30. H. Shen, H. Wang, X. Li, H. Wang, X. Chen, L. S. Li, *Dalton Trans.,* **2009**, *47*, 10534.

31. S. Gul, J. K. Cooper, P. Glans, J. Guo, V. K. Yachandra, J. Yano, J. Z. Zhang, *ACS Nano*, **2013**, *7*, 8680.

32. Z. Tan, Y. Zhang, C. Xie, H. Su, J. Liu, C. Zhang, N. Dellas, S. E. Mohney, Y. Wang, J. Wang, J. Xu, *Adv. Mater.,* **2011**, *23*, 3553.

33. J. Lim, M. Park, W. K. Bae, D. Lee, S. Lee, C. Lee, K. Char, *ACS Nano,* **2013**, *7*, 9019.

34. R. Xie, U. Kolb, J. Li, T. Basché, A. Mews, *J. Am. Chem. Soc,* **2005**, *127*, 7480.

35. B. O. Dabbousi, J. RodriguezViejo, F. V. Mikulec, J. R. Heine, H. Mattoussi, R. Ober, K. F. Jensen, M. G. Bawendi, *J. Phys. Chem. B,* **1997**, *101*, 9463.

36. K. L. Victor, H. Robert, *J. Am. Chem. Soc.,* **1950**, *72*, 4847.

37. M. D. Clark, S. K. Kumar, J. S. Owen, E. M. Chan, *Nano Lett.,* **2011**, *11*, 1976.

38. D. S. Thakare, S. K. Omanwar, P. L. Muthal, S. M. Dhopte, V. K. Kondawar, S. V. Moharil, *Phys. Stat. Sol.,* **2004**, *201*, 574.

39. W. Ji, P. Jing, W. Xu, X. Yuan, Y. Wang, J. Zhao, A. K.-Y. Jen, *Appl. Phys. Lett.,* **2013**, *103*, 053106.

40. C. Ippen, T. Greco, Y. Kim, J. Kim, M. S. Oh, C. J. Han, A. Wedel, *Org. Electron.,* **2014**, *15*, 126.

41. C. Xiang, W. Koo, S. Chen, F. So, X. Liu, X. Kong, Y. Wang, *Appl. Phys. Lett.,* **2012**, *101*, 053303.

42. H. Shen, H. Wang, L. Qian, Y. Zheng, L. S. Li, *ACS Appl. Mater. Interfaces,* **2013**, *5*, 12011.

43. H. Shen, S. Wang, H. Wang, J. Niu, L. Qian, Y. Yang, A. Titov, J. Hyvonen, Y. Zheng, L. S. Li, *ACS Appl. Mater. Interfaces,* **2013**, *5*, 4260.